Exchange Narrowing: Magnetic Resonance Line Shapes and Spin Correlations in Paramagnetic $KMnF_3$, $RbMnF_3$, and MnF_2†

J. E. GULLEY, DANIEL HONE, D. J. SCALAPINO, AND B. G. SILBERNAGEL
Physics Department, University of California, Santa Barbara, California 93106
(Received 19 August 1969)

Analyses of line shapes and correlation functions are made to investigate the Mn^{++} EPR and F^{19} NMR in MnF_2, $KMnF_3$, and $RbMnF_3$. Quantitative comparison of theory and experiment is now possible for these systems, and the standard theoretical approximations have proven to be inadequate. However, the form of the exchange interaction and broadening mechanisms is simple enough to allow us to extend earlier work by calculating higher-order moments and higher-order times in the short-time expansion of the correlation function than are usually feasible. We investigate several model line profiles consistent with the second and fourth moments for EPR in the infinite temperature limit. Agreement with experimental linewidths is obtained only for line shapes whose wing structure is non-Lorentzian, in contrast to the truncated Lorentzian forms usually adopted. The correlation functions characteristic of these profiles are obtained for the purpose of comparison with direct calculations later. We present short-time expansions (to fourth order) of the correlation functions, and we find that they decay more slowly than the Gaussian form usually assumed. The NMR correlation can be obtained for all times by a small interpolation between the short-time solutions and the predictions of a diffusion model for long times. The resulting function is consistent with that obtained from the line-profile analysis and both are in substantial agreement with previous spin-correlation studies. The linewidths predicted from this analysis and the moment method are both in agreement with experiment.

I. INTRODUCTION

MAGNETIC-RESONANCE line shapes and linewidths in nonmagnetic insulators have been satisfactorily interpreted and, at least in some instances, quantitative agreement between experiment and theory has been obtained.[1,2] However, a similar detailed study of resonance profiles in strongly exchange-coupled paramagnetic solids has not been made. Although the fundamental processes of exchange narrowing are understood, inadequate knowledge of the relevant parameters (e.g., exchange constants) has precluded such a quantitative comparison. Recent precise measurements of the exchange constants in rutile MnF_2 and perovskite $KMnF_3$, $RbMnF_3$ make possible a direct application of exchange-narrowing theory yielding unambiguous predictions for the linewidths. However, there is a systematic discrepancy between the predictions of the theory in its simplest form and F^{19} NMR and Mn^{++} EPR experimental linewidths which substantially exceeds the uncertainties of either the calculated or measured quantities.[3] A more detailed application of the theory can account for the discrepancy.

There are two essentially equivalent approaches to the problem of exchange-narrowed linewidths, each with its own set of assumptions and limitations. In the moment method, as developed by Waller and Van Vleck,[1] various even moments ($M_2, M_4, \ldots$) of a symmetrical profile $I(\omega)$ are calculated. The line would be determined uniquely only if all moments were known. The labor involved in computing more than the first one or two, however, generally prevents a precise determination of the shape. It is customary, therefore, to *assume* a line profile whose parameters are characterized by the moments available.

In the linear-response theories of Anderson and Weiss (A-W),[4,5] and Kubo and Tomita (K-T),[6] $I(\omega)$ is shown to be the frequency Fourier transform of the magnetization correlation function $\langle M_x(t)M_x(0)\rangle$, which is commonly called the relaxation function $\varphi(t)$. Under very general circumstances,[7] the correlation function of the local field

$$\psi(\tau)=\frac{\langle\omega(\tau)\omega(0)\rangle}{\langle\omega(0)^2\rangle}, \quad \omega(t)=\gamma H_{\rm loc}(t) \tag{1.1}$$

is related to $\varphi(t)$ by

$$\varphi(t)=\exp\left[-\langle\omega(0)^2\rangle\int_0^t(t-\tau)\psi(\tau)d\tau\right]. \tag{1.2}$$

Then, if $\psi(\tau)$ decays much faster than $\varphi(t)$, this relation implies a resonance line which has Lorentzian shape, at least near its center, *regardless of the precise form of* $\psi(\tau)$. However, in order to extract more detailed information concerning the shape of the line and, in particular, its width, we must adopt an analytic form for $\psi(\tau)$. A full calculation of $\psi(\tau)$ is extremely difficult and it has been customary to approximate it by finding the leading terms in a short-time expansion and using the results to characterize an *assumed* form for $\psi(\tau)$. The accurate determination of $\psi(\tau)$ is a central difficulty in this approach to exchange-narrowing theory.

† Supported in part by the National Science Foundation.
[1] J. H. Van Vleck, Phys. Rev. **74**, 1168 (1948).
[2] I. J. Lowe and R. E. Norberg, Phys. Rev. **107**, 46 (1957).
[3] J. E. Gulley, B. G. Silbernagel, and V. Jaccarino, J. Appl. Phys. **40**, 1318 (1969).
[4] P. W. Anderson and P. R. Weiss, Rev. Mod. Phys. **25**, 269 (1953).
[5] P. W. Anderson, J. Phys. Soc. Japan **9**, 316 (1954).
[6] R. Kubo and K. Tomita, J. Phys. Soc. Japan **9**, 888 (1954).
[7] R. Kubo, in *Fluctuation, Relaxation, and Resonance in Magnetic Systems*, edited by D. ter Haar (Plenum Press Inc., New York, 1962).

The MnF_2, $KMnF_3$, and $RbMnF_3$ systems are especially suitable for a study of this problem. They form simple lattices in which all necessary parameters are accurately known. Since the ground state of the Mn^{++} ion is an orbital singlet, single-ion anisotropy and anisotropic exchange effects are small; thus we may safely neglect them. The simplicity of the remaining isotropic exchange terms in the Hamiltonian greatly facilitates calculation of the moments and leading coefficients of the short-time expansion of $\psi(t)$. We find that the computations of M_2 and M_4 in the EPR case and M_2, M_4, and M_6 in the NMR case are algebraically tractable and involve only well-defined parameters. Previous studies of this problem have made use of only M_2 and M_4, or equivalently the t^2 coefficient in the $\psi(t)$ expansion. In the NMR case, the ability to calculate M_6 and the t^4 coefficient of $\psi(t)$ *exactly*, gives us greater flexibility in dealing with both the line profile and the initial behavior of $\psi(t)$. For EPR, a reasonable estimate of M_6 is also possible and we use this to study systematics of the exchange-narrowing process in this case, as well.

We have used the three available moments to investigate line shapes with three adjustable parameters. We find that only a restricted class of these gives substantial agreement with experiment. This type of moment analysis can be related directly to the linear-response theories by Eq. (1.2), which determines the correlation function $\psi(t)$ appropriate to a particular line shape [through its Fourier transform $\varphi(t)$]. This can be compared to forms of $\psi(t)$ which are calculated directly from linear-response theory. In the NMR case, $\psi(t)$ can be decomposed into autocorrelation functions and pair-correlation functions, and the short-time expansions of each of these can be evaluated explicitly to order t^4. We find that neither any of the individual autocorrelation components nor $\psi(t)$ as a whole is Gaussian (as is often assumed). Using the short-time expansion results and a diffusion model to characterize $\psi(t)$ at long time, we have been able to obtain a $\psi(t)$ which is in good agreement with that predicted by the moment analysis.

Explicit expressions for M_2, M_4, M_6 for NMR and M_2, M_4 with an estimate of M_6 for EPR are presented in Sec. II. In Sec. III, these moments are used to study three parameter profiles and the resulting linewidths are compared with experiment. The correlation functions appropriate to the profiles discussed in Sec. III are given in Sec. IV, and these are compared with $\psi(t)$ calculated from linear response theory. The results are summarized and discussed in Sec. V.

II. MOMENT CALCULATIONS

In our study of line shapes and correlation functions, we will use as fundamental input the limited exact information we can obtain. In particular, we make extended use of the moments of the resonance lines, which are given by closed expressions involving traces over quantum-mechanical operators once the Hamiltonian $\mathcal{H}$ has been specified.

One of the useful features of the MnF_2, $KMnF_3$, and $RbMnF_3$ systems we have chosen to study is the particularly simple form of the exchange Hamiltonian $\mathcal{H}_{ex}$. Because Mn^{++} is an orbital singlet ($^6S_{5/2}$), terms in the Hamiltonian representing crystal-field effects are small and an estimate of their contribution to the moments indicates that they may be neglected. Measurements of the magnitude of the EPR g shift[8] in these materials indicates that both symmetric and antisymmetric anisotropic exchange terms[9] may also be neglected. Therefore, we have chosen an isotropic Heisenberg form for $\mathcal{H}_{ex}$. The full Hamiltonian is then given by

$$\mathcal{H}=\mathcal{H}_0+\mathcal{H}_p+\mathcal{H}_{ex}.$$

Here, $\mathcal{H}_0$ is the Zeeman term with the static field (H_0) along the z axis. $\mathcal{H}_p$ represents the perturbation responsible for the homogeneous linewidth—a dipolar interaction ($\mathcal{H}_D$) in the EPR case and a hyperfine interaction ($\mathcal{H}_{HF}$) in the NMR case. The EPR Hamiltonian then has the form

$$\mathcal{H}^{EPR}=H_0\gamma_e\hbar\sum_i S_i^z+(\hbar\gamma_e)^2 \times\sum_{i>j}[\mathbf{S}_i\cdot\mathbf{S}_j-3(\mathbf{S}_i\cdot\hat{r}_{ij})(\mathbf{S}_j\cdot\hat{r}_{ij})]\times\frac{1}{|r_{ij}|^3}+\sum_{i>j}J_{ij}\mathbf{S}_i\cdot\mathbf{S}_j, \quad (2.1)$$

where γ_e is the electronic gyromagnetic factor, $\mathbf{S}$ is the electron spin, $\hat{r}_{ij}$ is a unit vector in the direction from spin i to j, and J_{ij} is the exchange coupling constant between spins i and j. The indices i and j are summed over the magnetic sites only. In the presence of strong exchange ($\mathcal{H}_{ex}\gg\mathcal{H}_D$), nonsecular terms in $\mathcal{H}_D$ contribute to the linewidth and therefore must be retained in moment calculations.[4,10] This is in contrast to the situation in diamagnetic systems where these terms must be excluded since they contribute to satellites rather than to the central line.[1] The NMR Hamiltonian takes the form

$$\mathcal{H}^{NMR}=H_0\gamma_n\hbar\sum_i I_i^z+\sum_{i,j}\mathbf{I}_i\cdot\mathbf{A}_{ij}\cdot\mathbf{S}_j+\sum_{j>k}J_{jk}\mathbf{S}_j\cdot\mathbf{S}_k, \quad (2.2)$$

where γ_n is the nuclear gyromagnetic factor and the index i is summed over nuclear spins, while j and k label electron spins. The hyperfine tensor $\mathbf{A}_{ij}$ is of the form $\mathbf{A}_{ij}\delta_{ij}$ for the nuclei of magnetic ions (e.g., Mn^{55} in MnF_2). If several magnetic ions contribute a (transferred) hyperfine interaction at the site i of a nonmagnetic nucleus, then j summed over contributing sites.

[8] S. Geschwind and V. Jaccarino (unpublished).
[9] T. Moriya, Progr. Theoret. Phys. (Kyoto) **16**, 23 (1956); **16**, 641 (1956).
[10] F. Keffer, Phys. Rev. **88**, 686 (1952).

In the infinite temperature limit, the second and fourth moments are given by[1]

$$\langle\omega^2\rangle=-\frac{1}{\hbar^2}\frac{\mathrm{Tr}[\mathcal{H},M^x]^2}{\mathrm{Tr}[M^x]^2},\quad \langle\omega^4\rangle=\frac{1}{\hbar^4}\frac{\mathrm{Tr}[\mathcal{H},[\mathcal{H},M^x]]^2}{\mathrm{Tr}[M^x]^2},\tag{2.3}$$

$$M^x=\gamma_e S^x \text{ for EPR},\quad M^x=\gamma_n I^x \text{ for NMR}.$$

Higher even moments are generated in a similar manner.

The first of the commutators above is

$$[\mathcal{H},M^x]=[\mathcal{H}_0,M^x]+[\mathcal{H}_p,M^x]+[\mathcal{H}_{ex},M^x].\tag{2.4}$$

Since the last term vanishes, exchange is not a broadening mechanism. The only effect of $[\mathcal{H}_0,M^x]$ is to establish the position for resonance ω_0. We are interested in the moments about ω_0, $\langle(\omega-\omega_0)^n\rangle$, and since $\mathcal{H}_0$ does not enter into their calculation, it will be neglected in what follows. Furthermore, $\mathcal{H}_{ex}\gg\mathcal{H}_0$, $\mathcal{H}_p$ so the dominant contributions to the fourth and sixth moments are given by the replacements

$$[\mathcal{H},[\mathcal{H},M^x]]\rightarrow[\mathcal{H}_{ex},[\mathcal{H}_p,M^x]];$$
$$[\mathcal{H},[\mathcal{H},[\mathcal{H},M^x]]]\rightarrow[\mathcal{H}_{ex},[\mathcal{H}_{ex},[\mathcal{H}_p,M^x]]].\tag{2.5}$$

A. EPR Moments

Calculation of M_2 with the full dipolar Hamiltonian taken as $\mathcal{H}_p$ yields (after use of the standard angular-momentum commutation relations,[11])

$$M_2=\gamma_e{}^4\hbar^2S(S+1)\tfrac{3}{2}\sum{}'B_{ij},\qquad B_{ij}=(1+\gamma_{ij}{}^2)|r_{ij}|^{-6}.\tag{2.6}$$

The sum is over j only and $j\neq i$. γ_{ij} is the direction cosine of r_{ij} relative to H_0. Eq. (2.6) is in agreement with previous results,[12] and its isotropic average is easily shown to be exactly 10/3 times the powder formula computed with a truncated dipolar Hamiltonian.[1]

The corresponding expression for M_4 is

$$M_4=\gamma_e{}^4S(S+1)\{(9/5)[S(S+1)-\tfrac{3}{4}]\times\sum_j{}'J_{ij}{}^2B_{ij}+S(S+1)\sum_{j\neq k}{}'[2J_{ij}J_{ik}C_{ij;ik}+J_{ij}J_{jk}(B_{ik}-4C_{ij;ik})+J_{ij}{}^2(2B_{ik}-4C_{ik;jk})]\},\tag{2.7}$$

where B_{ij} is defined above and

$$C_{ij;ik}=\{-\tfrac{1}{2}[\gamma_{ij}{}^2(1-2\gamma_{ik}{}^2)+\gamma_{ik}{}^2(1-2\gamma_{ij}{}^2)]+\tfrac{1}{2}(1-\gamma_{ij}{}^2)(1-\gamma_{ik}{}^2)\cos^2\xi+(\tfrac{5}{2})\gamma_{ij}\gamma_{ik}\times[(1-\gamma_{ij}{}^2)(1-\gamma_{ik}{}^2)]^{1/2}\cos\xi\}|r_{ij}|^{-3}|r_{ik}|^{-3}.\tag{2.8}$$

Here ξ is the angle between $\mathbf{r}_{ij}$ and $\mathbf{r}_{ik}$ projected onto the xy plane.

Again the sums are independent of i and are restricted to $i\neq j\neq k\neq i$. The isotropic average of M_4 cannot be made in general, since specific knowledge of the lattice is necessary in order to average the $C_{ij;ik}$ and $C_{ik;ij}$ terms.[13] If dipolar sums are restricted to near neighbors in cubic systems, this result reduces to the form given by Cooper and Keffer.[12] In the numerical calculations of EPR moments reported below, the sums in Eqs. (2.6) and (2.7) were evaluated over a volume, seven lattice constants on a side.

Explicit computation of the sixth and higher moments for EPR with the untruncated dipolar Hamiltonian becomes increasingly involved and we have not attempted it. However, it is possible to make a reasonable and useful estimate for M_6 for the cubic systems $KMnF_3$ and $RbMnF_3$. The sixth moment for a simple cubic system with H_0 in the [100] direction has been calculated taking $\mathcal{H}_p$ to be a truncated dipolar Hamiltonian[14]:

$$M_6{}^T(100)=(9/4)\gamma_e{}^4J^4\hbar^{-2}a^{-6}[520(S(S+1))^3-230(S(S+1))^2-14S(S+1)],\tag{2.9}$$

where a is the lattice constant and only highest-order terms in J have been retained. We assume that if $\mathcal{H}_p$ is untruncated $M_6\simeq(10/3)M_6{}^T(100)$. The correction factor 10/3 is expected to apply only for an isotropic average of $M_6{}^T$. Since $M_6{}^T$ is undoubtedly somewhat anisotropic, the value chosen here is not strictly correct. Analysis of $M_2{}^T$ and $M_4{}^T$ [1] indicates that the error involved in this assumption should not exceed a factor of 2.

B. NMR Moments: Magnetic Nucleus

These difficulties with the sixth moment are not as severe in the nuclear case, where the perturbation Hamiltonian is much simpler, and we have been able to calculate M_6 explicitly. Moment calculations for nuclear resonance fall into two groups: those pertaining to the resonance of the nucleus of the magnetic ion, and those for the nucleus of a nonmagnetic ion. The latter group is comprised of those nuclei which experience a transferred hyperfine interaction.

As mentioned above, $\mathcal{H}_p$ for the magnetic nucleus has the diagonal form

$$\mathcal{H}_p=\mathcal{H}_{HF}=\sum_{i\nu}A_{\nu\nu}I_i{}^\nu S_i{}^\nu,\tag{2.10}$$

where $\nu=x'$, y', z' represent the principal axes of the hyperfine tensor. We shall assume that H_0 is directed along the z' axis, which is appropriate for the systems studied.

The second moment is easily shown to be

$$M_2=\mathfrak{A}^2\hbar^{-2}[\tfrac{1}{3}S(S+1)],\tag{2.11}$$

where $\mathfrak{A}^2\equiv A_{z'z'}{}^2+\frac{1}{2}(A_{x'x'}{}^2+A_{y'y'}{}^2)$. The corresponding

[11] E. Ambler, J. C. Eisenstein, and J. F. Schooley, J. Math. Phys. **3**, 118 (1961).

[12] See, for example, B. R. Cooper and F. Keffer, Phys. Rev. **125**, 896 (1962).

[13] A. J. Buslik, thesis, University of Pittsburgh (unpublished).

[14] G. Ia. Glebashev, Zh. Eksperim. i Teor. Fiz. **32**, 82 (1957) [English transl.: Soviet Phys.—JETP **5**, 38 (1957)].

results for M_4 and M_6 are

$$M_4=2\mathcal{A}^2\hbar^{-4}[\tfrac{1}{3}S(S+1)]^2\sum{}'J_{ij}^2, \tag{2.12}$$

$$M_6=\frac{1}{\hbar^6}\mathcal{A}^2[\tfrac{1}{3}S(S+1)]^2\{(4S^2+4S-1)\sum{}'J_{ij}^4 +[\tfrac{1}{3}S(S+1)]\sum_{j\neq k}{}' (14J_{ij}^2J_{ik}^2-4J_{ij}J_{ik}^2J_{jk})\}, \tag{2.13}$$

where, as before, the index i is not summed and the primes restrict summation indices j, k to be unequal to i. For a two-sublattice antiferromagnet with only intersublattice exchange the $J_{ij}J_{ik}^2J_{jk}$ term in M_6 vanishes.

C. NMR Moments: Partially Magnetic Nucleus

In this case the resonant nucleus of a nonmagnetic ion is coupled to adjacent electron spins through an effective hyperfine interaction

$$\mathcal{H}_{\mathrm{HF}}=\sum_{i,j}\mathbf{I}_i\cdot\mathbf{A}_{ij}\cdot\mathbf{S}_j. \tag{2.14}$$

The index i labels the nonmagnetic resonant sites and j refers to the magnetic sites. In MnF_2, for example, a given F^{19} nucleus is coupled via a transferred hyperfine interaction to three neighboring manganese sites. In $KMnF_3$ and $RbMnF_3$, the fluorines are involved in a similar interaction with two manganese ions, as shown in Fig. 1.

We shall assume that each resonant nucleus interacts with n equivalent neighboring spins. The moments are generated as in the case of the magnetic nucleus except for the manner in which the sites are enumerated. The results are

$$M_2=(1/\hbar^2)[\tfrac{1}{3}S(S+1)]n\mathcal{A}^2, \tag{2.15a}$$

$$M_4=(2\mathcal{A}^2/\hbar^4)[\tfrac{1}{3}S(S+1)]^2\sum_{\alpha,l}J_{\alpha l}^2, \tag{2.15b}$$

$$M_6=(\mathcal{A}^2/\hbar^6)[\tfrac{1}{3}S(S+1)]^2\{(4S^2+4S-1)\sum_{\alpha,l}J_{\alpha l}^4 +[\tfrac{1}{3}S(S+1)]\sum_{\alpha\neq\beta,l}(10J_{\alpha l}^2J_{\beta l}^2+4J_{\alpha l}^2J_{\alpha\beta}^2 -4J_{\alpha l}^2J_{\beta l}J_{\alpha\beta})+[\tfrac{1}{3}S(S+1)] \times\sum_{\alpha,l\neq m}(10J_{\alpha l}^2J_{\alpha m}^2+4J_{\alpha l}^2J_{lm}^2-4J_{\alpha l}J_{\alpha m}J_{lm}^2)\}, \tag{2.15c}$$

where $\alpha, \beta=1, 2,\ldots, n$; $l, m=n+1,\ldots, N$, and N is the total number of magnetic sites. The l, m sums are restricted to spins outside of the cluster, because $[J_{lm}\mathbf{S}_l\cdot\mathbf{S}_m, \sum_{\alpha=1}^{n}\mathbf{S}_\alpha]=0$ for $l, m\leq n$. In the special case $n=1$, the expressions reduce to the corresponding moments for the magnetic nucleus.

It is useful to dispaly the explicit forms of Eq. (2.15) appropriate to the F^{19} nucleus in MnF_2, $KMnF_3$, and $RbMnF_3$. The local environments of the F^{19} nucleus and the unit cells of these systems are shown in Fig. 1. In MnF_2 the F^{19} couples by $A_{\nu\nu}^{\mathrm{I}}$ to two Mn^{++} ions and by $A_{\nu\nu}^{\mathrm{II}}$ to one Mn^{++} ion. We shall neglect the small ($<2\%$) difference between $\mathcal{A}^{\mathrm{I}}$ and $\mathcal{A}^{\mathrm{II}}$. These magnetic ions form a body-centered tetragonal lattice with next-nearest-neighbor exchange. In $KMnF_3$ and $RbMnF_3$, the fluorines couple to two equivalent Mn^{++} ions which form corners of a simple cubic magnetic lattice with nearest-neighbor exchange. Explicit calculation of the sums indicated in Eq. (2.15) for these special cases are listed in Table I.

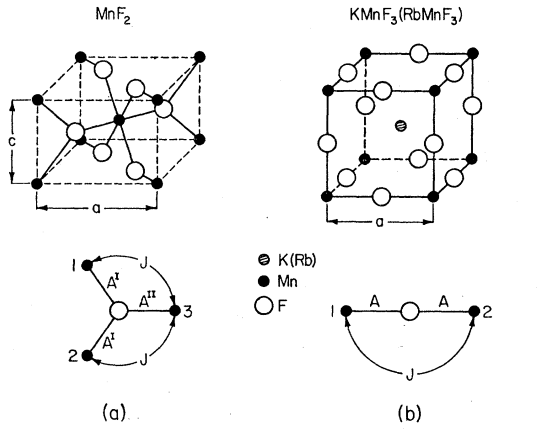

FIG. 1. Unit cells for rutile (a) and cubic perovskite (b) structures. Below each is shown the local environment of a F^{19} nucleus. Hyperfine and exchange interactions are indicated explicitly.

The necessary parameters and numerical values for the moments as given by Eqs. (2.6)–(2.8) and Table I are listed in Table II. Errors assigned to the moments are the result of the indicated uncertainities in the physical constants. These moments are applied below in the discussion of line shapes and correlation functions.

III. MODEL LINE SHAPES

Having determined the first few moments of the NMR and EPR lines, we are now in a position to study possible resonance line shapes $I(\omega)$. In this section, we consider some model line shapes consistent with experiment and with the calculated moments. In the strongly exchange-narrowed limit, the truncated Lorentzian profile has generally been adopted for two main reasons. First, experimental line shapes are Lorentzian within the observable region. Second, since this profile is completely characterized by two parameters, the linewidth

TABLE I. NMR moments for F^{19} in MnF_2, $KMnF_3$, and $RbMnF_3$.

$MnF^{19}{}_2$	$KMnF^{19}{}_3$, $RbMnF^{19}{}_3$
$M_2=3\mathcal{A}^2\hbar^{-2}[\frac{1}{3}S(S+1)]$	$2\mathcal{A}^2\hbar^{-2}[\frac{1}{3}S(S+1)]$
$M_4=40\mathcal{A}^2J^2\hbar^{-4}[\frac{1}{3}S(S+1)]^2$	$20\mathcal{A}^2J^2\hbar^{-4}[\frac{1}{3}S(S+1)]^2$
$M_6=20\mathcal{A}^2J^4\hbar^{-6}[\frac{1}{3}S(S+1)]^2$ $\times\{104[\frac{1}{3}S(S+1)]-1\}$	$10\mathcal{A}^2J^4\hbar^{-6}[\frac{1}{3}S(S+1)]^2$ $\times\{76[\frac{1}{3}S(S+1)]-1\}$

TABLE II. Physical parameters and moments. Hyperfine constants are calculated according to definition given below Eq. (2.11).

	MnF_2	$RbMnF_3$	$KMnF_3$
Physical parameters			
lattice (Å)	$a=4.87$	$a=4.24$	$a=4.19$
	$c=3.31$		
J(°K)	3.52±0.03[a]	6.8 ±0.6[b]	7.60±0.08[c]
$\mathfrak{a}(10^{-4}$ cm$^{-1})$	I 22.56±0.22[d]	24.83±0.81[e]	25.67±0.41[f]
	II 23.00±0.32		
Moments			
NMR:			
$M_2(10^{18}$ sec$^{-2})$	1.59±0.03	1.27±0.08	1.36±0.04
$M_4(10^{43}$ sec$^{-4})$	1.31±0.03	2.93±0.54	3.92±0.14
$M_6(10^{68}$ sec$^{-6})$	4.21±0.18	25.8 ±9.2	42.8 ±2.2
EPR:			
$M_2(10^{21}$ sec$^{-2})$	10.30	2.68	2.88
$M_4(10^{47}$ sec$^{-4})$	1.99±0.04	1.00±0.17	1.34±0.02
$M_6(10^{73}$ sec$^{-6})$	···	≃3[g]	≃5[g]

[a] C. Trapp and J. W. Stout, Phys. Rev. Letters **10**, 157 (1953).
[b] C. G. Windsor and R. W. H. Stevenson, Proc. Phys. Soc. (London) **87**, 501 (1966).
[c] S. J. Pickart, M. F. Collins, and C. G. Windsor, J. Appl. Phys. **37**, 1054 (1966).
[d] A. M. Clogston, J. P. Gordon, V. Jaccarino, M. Peter, and L. R. Walker, Phys. Rev. **117**, 1222 (1960).
[e] M. B. Walker and R. W. H. Stevenson, Proc. Phys. Soc. (London) **87**, 35 (1966).
[f] R. G. Shulman and K. Knox, Phys. Rev. **119**, 94 (1960).
[g] This value is an estimate based upon Eq. (2.9), see text.

(δ_L) and the cutoff frequency (α), only two moments (M_4 and M_2) are required. In these systems, the cutoff occurs at frequencies of the order of the exchange frequency, which is thousands of times the linewidth, so the assumed Lorentzian shape extends far into the wings and outside the region of observation, where it is finally abruptly terminated. This model correctly describes the central portion of the line, and it has been customarily assumed that such parameters as the linewidth do not depend strongly on the particular details of its high-frequency cutoff. However, the fourth and higher moments are increasingly sensitive to this region of the line. The functional form of $I(\omega)$ far in the wings therefore does significantly affect the manner in which the calculated moments are related to the linewidth, contrary to the usual assumption. An infinite number of moments is required to completely describe the entire line, whereas only the calculation of the first few is mathematically practical. However, it seems reasonable to make whatever adjustments are possible to the wing structure of the line within the restrictions of the first three moments we have computed. This means that we may choose profiles with three adjustable parameters.

The model lines must conform to two general requirements. They must be very nearly Lorentzian within the experimentally accessible region, and they must have finite moments if they are to represent physical line shapes. As an initial example consider a two parameter "Gaussian-Lorentzian" (GL) profile

$$I^{\mathrm{GL}}(\omega)=(\delta/\pi)\exp[-(\omega/\alpha)^2]/(\delta^2+\omega^2). \tag{3.1}$$

Here, α should be characteristic of exchange frequencies. Thus, $\alpha\gg\delta$ and $I^{\mathrm{GL}}(\omega)$ is nearly Lorentzian at the center but the wing structure falls off continuously rather than being abruptly terminated. If terms of order δ/α are neglected, this profile yields

$$M_2=\alpha\delta/\pi^{1/2},\quad M_4=\tfrac{1}{2}\alpha^3\delta/\pi^{1/2},\quad \alpha/\delta=2\pi^{-1/2}M_4/M_2{}^2. \tag{3.2}$$

In these systems $M_4/M_2{}^2\simeq 10^3$–10^4, so the condition $\alpha\gg\delta$ is well satisfied. Solving for δ, we find that

$$\delta^{\mathrm{GL}}=(\tfrac{1}{2}\pi)^{1/2}M_2{}^{3/2}/M_4{}^{1/2}. \tag{3.3}$$

In Sec. IV, we show that this GL profile is equivalent to the assumption of a Gaussian form for $\psi(t)$. These results are to be contrasted with those of a truncated Lorentzian (TL)[15]

$$M_2{}^{\mathrm{TL}}=2\alpha\delta/\pi,\quad M_4{}^{\mathrm{TL}}=2\alpha^3\delta/3\pi,\quad \delta^{\mathrm{TL}}=(\tfrac{1}{2}\pi/\sqrt{3})M_2{}^{3/2}/M_4{}^{1/2}, \tag{3.4}$$

where α is the truncation frequency. Equation (3.3) leads to a width $(6/\pi)^{1/2}$ larger than that given by Eq. (3.4). However, both δ^{GL} and δ^{TL} severely underestimate the experimental linewidth. We seek a profile which is more consistent with experiment. Initial investigations of three-parameter line shapes[16] have indicated that only a restricted class will accomplish this. The appropriate shape is Lorentzian near ω_0, but then passes through an extended region approaching a $1/\omega^4$ frequency dependence before falling off in a manner so as to preserve finite moments. Deviations from a Lorentzian form are understood to occur far into the wings and outside the region of observation.

To illustrate this technique and explore the sensitivity to the details of the wing structure, we shall consider two such three-parameter line shapes which are analogous to TL and GL discussed above. A simple form with the desired functional dependence in the wings but with abrupt termination is the "truncated double Lorentzian" (TDL) given as

$$I^{\mathrm{TDL}}(\omega)=(\delta\alpha'^2/\pi)[(\omega^2+\delta^2)(\omega^2+\alpha'^2)]^{-1},\quad \omega<\alpha''$$
$$=0,\quad \omega>\alpha'' \tag{3.5}$$

where again α' and α'' are of the order of exchange frequencies so that $\alpha''>\alpha'\gg\delta$. As for the simpler line shapes, the three parameters $(\delta,\alpha',\alpha'')$ can be related to the moments (M_2,M_4,M_6) where

$$M_2=\alpha'\delta A(\eta),\quad M_4=(2/\pi)\delta\alpha'^2\alpha'' B(\eta),\quad M_6=(2\delta/3\pi)\alpha'^2\alpha''^3 C(\eta),$$

with

$$A(\eta)=(2/\pi)\tan^{-1}(1/\eta),\quad B(\eta)=1-\eta\tan^{-1}(1/\eta),\quad C(\eta)=1-3\eta^2+3\eta^3\tan^{-1}(1/\eta),\quad \eta=\alpha'/\alpha''. \tag{3.6}$$

[15] See, for example, A. Abragam, *The Principles of Nuclear Magnetism* (Oxford University Press, New York, 1961), p. 107.
[16] J. E. Gulley, B. G. Silbernagel, and V. Jaccarino, Phys. Letters **29A**, 657 (1969).

TABLE III. Cutoff and linewidth parameters of model line shapes, as defined in Eqs. (3.1), (3.5), and (3.9).

	NMR			EPR		
	MnF_2	$RbMnF_3$	$KMnF_3$	MnF_2	$RbMnF_3$	$KMnF_3$
δ^{exp}(G)	37.2 ±1	19.7 ±1	19.5 ±1	260 ±10	58 ±3	59 ±3
TL						
δ^{TL}(G)	19.9 ±0.5	9.5 ±1.0	9.1 ±0.3	120.8 ±1.2	22.6 ±2.5	21.8 ±0.7
$\alpha^{TL}(10^{12}\ sec^{-1})$	4.97±0.05	8.3 ±0.7	9.3 ±0.1	7.61±0.07	10.6 ±0.9	11.8 ±0.11
GL						
δ^{GL}(G)	27.5 ±0.7	13.2 ±1.4	12.6 ±0.4	165.9 ±3.3	31.2 ±3.4	30.0 ±1.0
$\alpha^{GL}(10^{12}\ sec^{-1})$	4.06±0.04	6.8 ±0.6	7.59±0.07	6.21±0.06	8.63±0.7	9.64±0.10
TDL						
δ^{TDL}(G)	40.4 ±1.0	19.0 ±1.9	18.1 ±0.6		72[a]	69[a]
$\alpha'(10^{12}\ sec^{-1})$	1.80±0.02	3.03±0.26	3.46±0.03		2.2	2.5
$\alpha''(10^{12}\ sec^{-1})$	8.70±0.09	14.4 ±1.3	16.0 ±0.2		28.4	31.7
$\eta=\alpha'/\alpha''$	0.21	0.21	0.22		0.08	0.08
GDL						
δ^{GDL}(G)	31.8 ±0.8	15.0 ±1.5	14.3 ±0.5		54	52
$\alpha'(10^{12}\ sec^{-1})$	3143±0.03	5.88±0.52	6.75±0.07		3.3	3.7
$\alpha''(10^{12}\ sec^{-1})$	6.01±0.06	9.90±0.9	10.95±0.1		22.0	24.5
$\eta=\alpha'/\alpha''$	0.57	0.59	0.61		0.15	0.15

[a] The values for GDL and TDL EPR are estimates because they involve the use of Eq. (2.9).

We assume α', $\alpha''\gg\delta$, but have retained all orders in η, since α' and α'' may have comparable magnitudes. From Eq. (3.6) we have

$$\delta^{TDL}=\frac{2\sqrt{3}}{\pi}\frac{M_6^{1/2}M_2^2}{M_4^{3/2}}\frac{B(\eta)^{3/2}}{C(\eta)^{1/2}A(\eta)^2}, \tag{3.7}$$

where η is determined self-consistently by

$$\eta=\tfrac{1}{6}\pi(M_4^2/M_2M_6)[A(\eta)C(\eta)/B(\eta)^2]. \tag{3.8}$$

We shall compare the characteristics of this line with one whose wing structure is smoothed out, avoiding the abrupt termination. We propose the "Gaussian double-Lorentzian" line (GDL)

$$I^{GDL}(\omega)=\frac{\delta}{\pi}\frac{\alpha'^2\exp[-(\omega/\alpha'')^2]}{(\omega^2+\delta^2)(\omega^2+\alpha'^2)}. \tag{3.9}$$

Proceeding as with TDL, we obtain

$$M_2=\delta\alpha' a(\eta),\quad M_4=\delta\pi^{-1/2}\alpha'^2\alpha'' b(\eta),$$
$$M_6=\tfrac{1}{2}\delta\pi^{-1/2}\alpha'^2\alpha''^3 c(\eta),$$
$$a(\eta)=e^{\eta^2}\mathrm{erfc}(\eta),\quad b(\eta)=1-\pi^{1/2}\eta e^{\eta^2}\mathrm{erfc}(\eta)$$
$$c(\eta)=1-2\eta^2+2\pi^{1/2}\eta^3 e^{\eta^2}\mathrm{erfc}(\eta), \tag{3.10}$$
$$\delta^{GDL}=\left(\frac{2}{\pi}\right)^{1/2}\frac{M_6^{1/2}M_2^2}{M_4^{3/2}}\frac{b(\eta)^{3/2}}{c(\eta)^{1/2}a(\eta)^2},$$
$$\eta=\left(\frac{\pi}{2}\right)^{1/2}\frac{M_4^2}{M_2M_6}\frac{a(\eta)c(\eta)}{b(\eta)^2}.$$

It should be noted that there is no necessary relation between the values of η for these two profiles.

The cutoffs and linewidth parameters of the four model line shapes, as determined by the calculated moments, are given in Table III for NMR and EPR in MnF_2, $KMnF_3$, and $RbMnF_3$. The experimental values of δ are included for comparison. We point out that the more flexible three-parameter forms (TDL and GDL) exhibit an extended region ($\alpha'\leq\omega\leq\alpha''$) of non-Lorentzian behavior. In Table IV, where the ratios of experimental to theoretical values of δ are presented, we find that these same profiles give improved agreement with the observed linewidths. It is perhaps surprising that TDL gives substantially better agreement than GDL; this will be discussed further in Sec. V.

We believe that the above analysis represents more than simple curve fitting. The results can be shown to be consistent with a study of the related correlation functions, which is the subject of Sec. IV.

IV. CORRELATION FUNCTIONS

In principle, it is possible to determine the correlation function $\psi(t)$ corresponding to any $I(\omega)$. The Fourier transform of $I(\omega)$ is the relaxation function $\varphi(t)$ which is related to $\psi(t)$ by Eq. (1.2). Differentiation of that equation gives

$$\psi(t)=[(\dot{\varphi}^2/\varphi^2)-(\ddot{\varphi}/\varphi)]/\langle\omega(0)^2\rangle. \tag{4.1}$$

The calculational difficulties then all lie with performing the Fourier transformation of $I(\omega)$. Eq. (4.1) can be simplified in the limit of strong exchange narrowing when $\psi(t)$ decays in a time of order $\hbar/J$ (J is the exchange constant). In this large J limit $\hbar/J$ is much less

TABLE IV. Ratios of experimental to theoretical linewidth for various model profiles.

	NMR			EPR		
	MnF_2	$RbMnF_3$	$KMnF_3$	MnF_2	$RbMnF_3$	$KMnF_3$
δ^{exp}/δ^{TL}	1.87	2.07	2.14	2.15	2.57	2.71
δ^{exp}/δ^{GL}	1.35	1.49	1.55	1.57	1.85	1.97
$\delta^{exp}/\delta^{GDL}$	1.17	1.31	1.36	···	1.07	1.13
$\delta^{exp}/\delta^{TDL}$	0.92	1.04	1.08	···	0.80	0.86

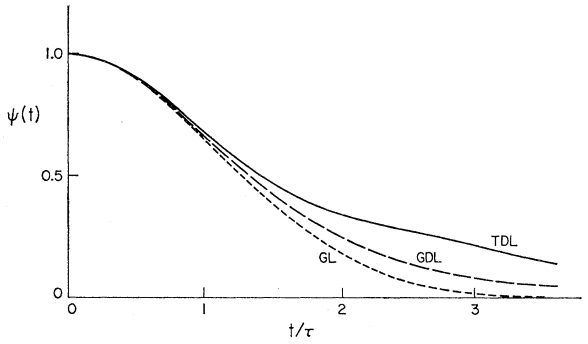

FIG. 2. Correlation functions for GL, GDL, TDL model line shapes appropriate to MnF_2. τ is defined in Eq. (4.24).

than the relaxation time characterizing $\varphi(t)$, and for $t\gg\hbar/J$, Eq. (1.2) may be written[5] approximately as

$$\varphi(t)\approx\exp\left[-\langle\omega(0)^2\rangle t\int_0^\infty\psi(\tau)d\tau\right]. \tag{4.2}$$

It is convenient to set the time scale of $\psi(t)$ by the integral in Eq. (4.2) rather than by $\hbar/J$. We make the conventional definition of an exchange frequency ω_e as

$$\frac{1}{\omega_e}\equiv\int_0^\infty\psi(\tau)d\tau. \tag{4.3}$$

Thus, $\varphi(t)$ decays in a time of order $\omega_e/\langle\omega(0)^2\rangle$. Since $\psi(t)$ is negligible after times of order $1/\omega_e\ll\omega_e/\langle\omega(0)^2\rangle$, we can simplify Eq. (4.1) by the approximations $\varphi(t)\approx\varphi(0)$, $\dot\varphi(t)\approx0$,

$$\psi(t)\simeq-\ddot\varphi(t)/[\varphi(0)\langle\omega(0)^2\rangle]. \tag{4.4}$$

For the GL profile, $\varphi(t)$ can be obtained analytically as

$$\varphi(t)/\varphi(0)=\{e^{-\delta t}\mathrm{erfc}[(\delta/\alpha)-\tfrac{1}{2}\alpha t]+e^{\delta t}\mathrm{erfc}\times[(\delta/\alpha)+\tfrac{1}{2}\alpha t]\}/2\mathrm{erfc}(\delta/\alpha). \tag{4.5}$$

where erfc is the complementary error function. Subsequent differentiation yields

$$\psi(t)/\psi(0)\simeq\exp[-\tfrac{1}{4}(\alpha t)^2], \tag{4.6}$$

where $\alpha^2=2M_4/M_2$ has been defined in Sec. III [Eq. (3.2)]. A similar analtyic expression can be obtained for the GDL profile

$$\psi(t)/\psi(0)\simeq\{e^{-\eta T}\mathrm{erfc}(\eta-\tfrac{1}{2}T)+e^{\eta T}\mathrm{erfc}(\eta+\tfrac{1}{2}T)\}/2\ \mathrm{erfc}\eta, \tag{4.7}$$

where $T=\alpha''t$. For the TL and TDL profiles, the expressions for $\psi(t)$ and $\psi(t)$ can be obtained numerically. The results of these calculations for the F^{19} NMR in MnF_2 are shown in Fig. 2, where the correlation functions for GL, GDL, and TDL profiles are shown explicitly. For $\omega_e t<1$, the three forms of $\psi(t)$ are nearly indistinguishable, but their behavior at longer times is substantially different; the TDL profile decays much less rapidly than the GL and GDL forms.

This behavior of $\psi(t)$ is directly related to the values of the linewidth determined in Sec. III. From Eq. (4.2), we see that $\varphi(t)$ is exponential except near $t=0$, so the central portion of $I(\omega)$ is Lorentzian with width $\delta=\langle\omega(0)^2\rangle/\omega_e$. Thus, δ is proportional to $1/\omega_e$, which from Eq. (4.3) is equal to the area under the $\psi(t)$ curve. A comparison of the magnitudes of δ given in Table II and the forms of $\psi(t)$ shown in Fig. 2 verifies that the TDL profile, which predicts the largest values of δ, also has the largest value of $\int\psi(\tau)d\tau$ by virtue of the slow decay of $\psi(t)$ for $t>1/\omega_e$.

A. Correlation Function

We would like to compare the $\psi(t)$ obtained from the line-shape analysis with direct calculations from linear-response theory. As with the moments, we can obtain in practice only a limited amount of explicit information about $\psi(t)$, namely, the coefficients of the leading terms of its small-time expansion. Again, the simplicity of the Hamiltonian for these systems enables us to carry this analysis further than previous workers have, and to check the validity of their assumed forms for $\psi(t)$. It is obvious from Fig. 2 that it will also be necessary to exercise some care in determining the long-time behavior of $\psi(t)$. Although an exact calculation is not possible in this instance, it is known that a diffusion model gives a good approximation to the spin dynamics. We show in Sec. IV C that only a short interpolation is required to connect the results to the short-time expansion, so that $\psi(t)$ is well determined for all t.

The short-time behavior of $\psi(t)$ is directly related[5] to the moments of $I(\omega)$, again through Eq. (1.2), since

$$(-i)^n\frac{d^n}{dt^n}\varphi(t)\bigg|_{t=0}=\int_{-\infty}^\infty\omega^nI(\omega)d\omega\Big/\int_{-\infty}^\infty(\omega)Id\omega=M_n. \tag{4.8}$$

Thus, successive differentiation of Eq. (1.2) gives

$$\langle\omega(0)^2\rangle=M_2, \tag{4.9a}$$

$$\ddot\psi(0)=-(M_4/M_2)+3M_2, \tag{4.9b}$$

$$\psi^{(\mathrm{IV})}(0)=(M_6/M_2)-15M_4+30M_2^2. \tag{4.9c}$$

If all moments where known, $\psi(t)$ would be determined exactly. Since only M_2 and M_4 have been generally available, it has been necessary to assume particularly simple forms for $\psi(t)$. A common assumption has been the Gaussian $\psi(t)=\exp(-\frac{1}{4}\pi\omega_e^2t^2)$, where ω_e is defined in Eq. (4.3). It is then found that[4]

$$\omega_e^2\simeq(2/\pi)(M_4/M_2),\quad\delta=(\tfrac{1}{2}\pi)^{1/2}(M_2^{3/2}/M_4^{1/2}). \tag{4.10}$$

We point out that the GL-model line profile implies precisely this $\psi(t)$ [see Eq. (4.6)], and the linewidth δ^{GL} of Eq. (3.3) is therefore identical to δ in Eq. (4.10).

The first few moments are thus sufficient to determine the parameters $\langle\omega(0)^2\rangle$ and ω_e. Since we have evaluated M_6, it is now possible to check the validity of the Gaussian assumption for $\psi(t)$. The short-time expansion of $\psi(t)$ can be written in the form

$$\psi(t)=1-\frac{1}{2!}\alpha t+\frac{1}{4!}\beta t^4\cdots, \tag{4.11}$$

where $\alpha=-\ddot{\psi}(t)|_{t=0}$, $\beta=\psi^{\mathrm{IV}}(t)|_{t=0}$, are given in terms of the moments by Eq. (4.9). If $\psi(t)$ were Gaussian, β/α^2 would be identically equal to 3. In the limit of strong exchange narrowing $\alpha\simeq+M_4/M_2$, $\beta\simeq M_6/M_2$, so $\beta/\alpha^2=M_2M_6/M_4^2$ provides a useful test for the Gaussian form. Using the explicit values for the NMR moments given in Table II, α, β, and β/α^2 are obtained for MnF_2 and $KMnF_3$, and are listed in Table V. Since $\beta/\alpha^2>3$, $\psi(t)$ decays more slowly than a true Gaussian as our earlier line-shape analysis leads us to expect. The estimate of the EPR sixth moment is not considered sufficiently reliable to be used in this rather sensitive test. The near equivalence of the two values of β/α^2 suggests that this ratio is characteristic of short-range, isotropic exchange interactions. This point will be explored further in Sec. V.

B. Autocorrelation and Pair-Correlation Functions

$\psi(t)$ is the correlation function of the full local field, which is in general the sum of contributions from many spins. Thus, $\psi(t)$ represents a combination of all possible correlation functions between pairs of these spins (including the autocorrelation functions). It is often helpful to calculate these components of $\psi(t)$ separately.

For NMR, the analysis is particularly simple, becasue local fields arise almost entirely from the short-range hyperfine interaction, and only a few spins are involved. Then, $\psi(t)$ is composed of the small number of correlation functions between pairs of these spins. The local field at a nuclear site may be written as

$$\mathbf{H}_i^{\mathrm{loc}}=(1/\gamma_n\hbar)\sum\overleftrightarrow{A}_{ij}\cdot\mathbf{S}_j, \tag{4.12}$$

where the j sum extends only over the magnetic spins which are neighbors to site i. Formally, the correlation function may be written as

$$\psi(t)=\langle\mathbf{H}_i^{\mathrm{loc}}(t)\cdot\mathbf{H}_i^{\mathrm{loc}}(0)\rangle/\langle\mathbf{H}_i^{\mathrm{loc}}(0)\cdot\mathbf{H}_i^{\mathrm{loc}}(0)\rangle,$$

where

$$\langle 0\rangle\equiv\mathrm{Tr}(e^{-\beta\mathcal{H}}0)/\mathrm{Tr}e^{-\beta\mathcal{H}}. \tag{4.13}$$

In the infinite-temperature limit the denominator is particularly simple since $\mathrm{Tr}S_i^{\mu}S_j^{\nu}=[\frac{1}{3}S(S+1)]\delta_{ij}\delta_{\mu\nu}$, where i, j are site indices and μ, ν are Cartesian components of the spin vector. The following discussion will be restricted to the infinite-temperature limit. If $\overleftrightarrow{A}_{ij}$ is the same for each j in the above sums, then Eq. (4.13) reduces to

$$\psi(t)=3\sum_{j,k}\langle S_j^z(t)S_k^z(0)\rangle/nS(S+1). \tag{4.14}$$

j, k are summed over the n magnetic sites contributing to the local field at i and $S_j^z(t)$ is a Heisenberg operator evolving in time according to the full Hamiltonian ($\mathcal{H}$). This assumption concerning $\overleftrightarrow{A}_{ij}$ is exactly satisfied in the perovskites and leads to small corrections in MnF_2.[17]

The numerator of Eq. (4.14) is a linear combination of autocorrelation ($j=k$) and pair-correlation functions ($j\neq k$). It is instructive to consider them separately.[18] The short-time expansion of each has the form

$$\langle S_i^z(t)S_j^z(0)\rangle=\langle S_i^zS_j^z\rangle+\frac{1}{2!}\alpha t^2+\frac{1}{4!}\beta t^4+\cdots, \tag{4.15}$$

where α and β are given by[9]

$$\alpha=\langle[\mathcal{H},S_j^z][S_k^z,\mathcal{H}]\rangle, \tag{4.16a}$$

$$\beta=\langle[\mathcal{H},[\mathcal{H},S_j^z]][[S_k^z,\mathcal{H}],\mathcal{H}]\rangle. \tag{4.16b}$$

In the case of strong exchange narrowing we may take $\mathcal{H}=\mathcal{H}_{\mathrm{ex}}$ in the above expressions.

For the nucleus of a magnetic ion, only the autocorrelation function is required because the hyperfine field is essentially produced by a single electron spin. Evaluation of Eq. (4.15) for $j=k$ (autocorrelation) yields

$$\langle S_j^zS_j^z\rangle=\tfrac{1}{3}S(S+1), \tag{4.17a}$$

$$\alpha_A=-2\hbar^{-2}[\tfrac{1}{3}S(S+1)]^2\textstyle\sum_k J_{jk}^2, \tag{4.17b}$$

$$\beta_A=\hbar^{-4}[\tfrac{1}{3}S(S+1)]^2\{(4S^2+4S-1)\sum_k J_{jk}^4+[\tfrac{1}{3}S(S+1)]\times\sum_{k\neq l}(10J_{jk}^2J_{jl}^2+4J_{jk}^2J_{kl}^2)\}. \tag{4.17c}$$

We have dropped terms such as $J_{jk}^2J_{jl}J_{kl}$ from β_A since they do not contribute in these simple antiferromagnets. Reference to the magnetic nucleus moment formulas [Eq. (2.11)–(2.13)] shows that

$$\alpha_A/[\tfrac{1}{3}S(S+1)]=-(M_4/M_2)^{\mathrm{Mag}}$$

and

$$\beta_A/[\tfrac{1}{3}S(S+1)]=(M_6/M_2)^{\mathrm{Mag}}$$

TABLE V. α, β and β/α^2 in the limit of strong exchange narrowing.

	MnF_2	$KMnF_3$
$\alpha(10^{24}\ \mathrm{sec}^{-2})$	8.24±0.08	28.8 ±0.30
$\beta(10^{50}\ \mathrm{sec}^{-4})$	2.65±0.05	31.47±0.63
β/α^2	3.9	3.8

[17] Although there are appreciable differences between the A_{ij} for different j in MnF_2, the combinations which appear as coefficients of the correlations are found to differ from each other by no more than a few percent.

[18] See, for example, B. G. Silbernagel, V. Jaccarino, P. Pincus, and J. H. Wernick, Phys. Rev. Letters **20**, 1091 (1968).

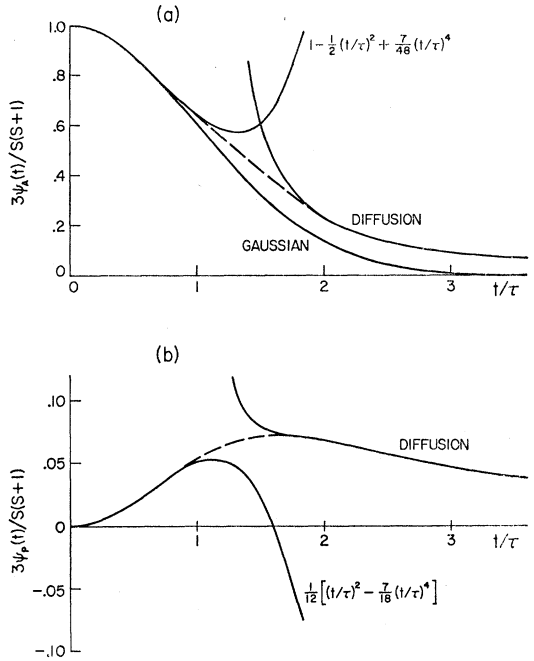

FIG. 3. Theoretical-autocorrelation (a) and pair-correlation (b) functions for $KMnF_3$. The interpolations between short-time expansions [Eqs. (4.24) and (4.25)] and the long-time asymptotic approximation (4.26) are shown dashed. The usual Gaussian approximation for the autocorrelation function is shown for comparison. The time scale is the same as in Fig. 2.

and we have verified that Eqs. (4.17) are in agreement with the general results (4.9).

For the nucleus of a nonmagnetic ion, pair correlations ($j\neq k$) among the spins in the cluster contributing to the hyperfine field must also be considered. These fall into two categories, those involving pairs within the cluster which are directly coupled by exchange (case 1) and those which are coupled only indirectly through intermediate spins (case 2). For type-1 pairs (j,k), $\langle S_j^z S_k^z\rangle=0$, and

$$\alpha_{P1}=2\hbar^{-2}J_{jk}^2[\tfrac{1}{3}S(S+1)]^2, \tag{4.18a}$$

$$\beta_{P1}=-[\tfrac{1}{3}S(S+1)]^2\hbar^{-4}\{J_{jk}^4(4S^2+4S-1)+[\tfrac{1}{3}S(S+1)]\times\textstyle\sum_l(20J_{jk}^2J_{jl}^2-6J_{jl}^2J_{kl}^2)\}. \tag{4.18b}$$

For type-2 pairs (j,k), where $J_{jk}=0$, $\langle S_j^z S_k^z\rangle=0$, $\alpha_{P2}=0$, and

$$\beta_{P2}=[\tfrac{1}{3}S(S+1)]^{-3}6\hbar^{-4}\textstyle\sum_l J_{jl}^2J_{kl}^2. \tag{4.19}$$

As a specific example, consider the $KMnF_3$ lattice shown in Fig. 1. For the Mn^{55} nucleus, only the autocorrelation function is required. For the F^{19} nucleus, two spins contribute equally to the nuclear hyperfine field and are directly coupled to each other by exchange. Thus,

$$\psi(t)=\langle\textstyle\sum_j S_j^z(t)\sum_k S_k^z\rangle=\langle(S_1^z(t)+S_2^z(t))(S_1^z+S_2^z)\rangle$$
$$=2\langle S_1^z(t)S_1^z(0)\rangle+2\langle S_1^z(t)S_2^z(0)\rangle \tag{4.20}$$

and $\psi(t)$ is characterized by two autocorrelation functions and two pair correlation functions of type 1. The coefficients of the expansions are

$$\begin{aligned}\alpha_A&=-2z[\tfrac{1}{3}S(S+1)]^2(J/\hbar)^2,\\ \beta_A&=(J/\hbar)^4[\tfrac{1}{3}S(S+1)]^2\\ &\quad\times z\{(4S^2+4S-1)+14(z-1)[\tfrac{1}{3}S(S+1)]\},\\ \alpha_{P1}&=2(J/\hbar)^2[\tfrac{1}{3}S(S+1)]^2,\\ \beta_{P1}&=-(J/\hbar)^4[\tfrac{1}{3}S(S+1)]^2\\ &\quad\times\{(4S^2+4S-1)+20(z-1)[\tfrac{1}{3}S(S+1)]\},\end{aligned} \tag{4.21}$$

where z is the coordination number (which is 6 for $KMnF_3$). As with the magnetic nucleus, by reference to the nonmagnetic nucleus formulas [Eq. (2.16)], it is easily shown that

$$(\alpha_A+\alpha_{P1})/[\tfrac{1}{3}S(S+1)]=-(M_4/M_2)^{\text{N-Mag}},$$
$$(\beta_A+\beta_{P1})/[\tfrac{1}{3}S(S+1)]=(M_6/M_2)^{\text{N-Mag}}.$$

Thus, for $KMnF_3$ and $RbMnF_3$, we again find agreement with the general results (4.9).

For the F^{19} nucleus in MnF_2, three autocorrelation terms appear. The pair correlation is more complicated because spins 1 and 3, and spins 2 and 3 are directly coupled by exchange (case 1) while spins 1 and 2 are only coupled through a spin such as 3 (case 2) (see Fig. 1). Thus,

$$\langle\textstyle\sum_j S_j^z(t)\sum_k S_k^z\rangle=3\langle S_1^z(t)S_1^z(0)\rangle+4\langle S_1^z(t)S_3^z(0)\rangle+2\langle S_1^z(t)S_2^z(0)\rangle. \tag{4.22}$$

Equation (4.21) is still applicable (with $z=8$) and we need in addition

$$\beta_{P2}=24(J/\hbar)^4[\tfrac{1}{3}S(S+1)]^3 \quad \text{for } MnF_2. \tag{4.23}$$

The sum of functions given above again correctly represents $\psi(t)$ in terms of $(M_4/M_2)^{\text{N-Mag}}$ and $(M_6/M_2)^{\text{N-Mag}}$ for MnF_2.

As was the case with the moment calculations, the particularly simple NMR Hamiltonians for these systems have made possible the explicit calculation of the t^4 coefficients (β's); whereas, usually it is only feasible to calculate the t^2 coefficients (α's). It is now possible, therefore, to compare the leading terms of the autocorrelation function with the Gaussian that has usually been assumed for this function.[9] Using α_A and β_A, we find that

$$\langle S_i^z(t)S_i^z(0)\rangle=[\tfrac{1}{3}S(S+1)]\left\{1-\frac{1}{2}\left(\frac{t}{\tau}\right)^2+\frac{7}{48}\left[1-\frac{1}{7z}\times\left(1+\frac{3}{2S(S+1)}\right)\right]\left(\frac{t}{\tau}\right)^4+\cdots\right\}, \tag{4.24}$$

where $(1/\tau)^2=2z(J/\hbar)^2[\frac{1}{3}S(S+1)]$. As was true for the full $\psi(t)$, the autocorrelation function decays less rapidly than a Gaussian. The expansion of the type-1 pair-

correlation function can be displayed similarly as

$$\langle S_i^z(t)S_j^z(0)\rangle_1 = \frac{1}{z}\frac{S(S+1)}{3} \times\left[\frac{1}{2!}\left(\frac{t}{\tau}\right)^2 - \frac{(5-2/z)}{4!}\left(\frac{t}{\tau}\right)^4 + \cdots\right]. \quad (4.25)$$

C. Long-Time Behavior

It is clear that if we are to make a quantitative comparison of calculated correlation functions with those generated from the model line shapes we must have specific information about their long-time behavior, whereas until now we have dealt only with short-time expansions. However, we can also determine approximately the long-time asymptotic behavior of $\psi(t)$, and it turns out that only a small interpolation is required to connect the short- and long-time approximations. If an exchange-coupled spin system is perturbed from its equilibrium condition at one site, the effects of this disturbance will propagate from the site in question by means of the exchange interaction. At a sufficiently long time after the initial perturbation, the effect will have involved a large number of spins; the original highly localized disturbance becomes one varying slowly over distances of the order of a lattice parameter. In this limit, the process may be characterized approximately as diffusion in an effective continuum of spins, in which case the correlation function $\psi(r,t) = 3\langle S_r^z(t)S_0^z(0)\rangle/S(S+1)$ obeys the equation

$$\Lambda\nabla^2\psi(r,t) = (\partial/\partial t)\psi(r,t). \quad (4.26)$$

The diffusion coefficient Λ has been calculated[19–21] in several different ways and the results of the more sophisticated theories[20,21] are in close agreement. At infinite temperature we know that $\psi(r,0) \propto \delta_{r0}$ (at equal times spins are uncorrelated for $T \to \infty$), but this cannot be used as a boundary condition on Eq. (4.26), since $\psi(r,t)$ varies too rapidly with position at short times for the continuum approximation to be valid. However, the Taylor series expansion in t/τ of parts A and B of this section is accurate in this time region. We have matched the long-time behavior to this by taking as the boundary condition for Eq. (4.26) the values of $\psi(r_j,t)$ given by the short-time expansions at roughly the maximum time for which these expansions can be trusted, $t/\tau = 1$. This gives

$$\psi(r,t) \approx [4\pi\Lambda(t-\tau)]^{-3/2}\sum_j \psi(r_j,\tau) \times\exp[-|\mathbf{r}_i-\mathbf{r}_j|^2/4\Lambda(t-\tau)], \quad t>\tau. \quad (4.27)$$

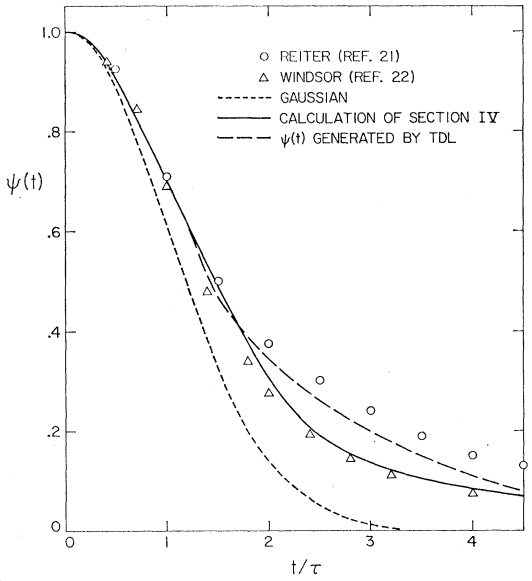

FIG. 4. The normalized correlation function for F^{19} NMR in $KMnF_3$. The appropriate combination (4.20) of the curves of Fig. 3 is compared with the form of $\psi(t)$ obtained from the TDL line shape (dashed line) and with the results of Refs. 21 and 22. The Gaussian approximation is again shown for comparison.

The resulting $\psi_A(t)$ ($r=0$) and $\psi_p(t)$ ($r=a$, where a is the near-neighbor distance) for $KMnF_3$ are given in Fig. 3. The short-dashed lines represent interpolations between the two limiting forms and the Gaussian approximation so $\psi_A(t)$ is shown for comparison. The correlation function of interest for the F^{19} NMR in $KMnF_3$, $\psi(t) = 2\psi_A(t) + 2\psi_p(t)$ is shown in Fig. 4. It is compared with the $\psi(t)$ obtained from the TDL study and with the Gaussian assumption for $\psi(t)$. Since the linewidth is proportional to $\int\psi(t)dt$, it is of interest to compare the area under these three $\psi(t)$ curves: GL = 1.25, TDL = 1.80, correlation analysis = 2.06 (in arbitrary units). The two latter values are within the experimental uncertainty of the observed linewidth ($\delta^{\text{exp}} = 1.94 \pm 0.15$ in these units). Both forms of the correlation function represent a substantial improvement over the Gaussian approximation for $\psi(t)$ (we point out again from Table III that the truncated Lorentzian line shape leads to even worse results). The TDL shape is too simple in form to give the long-time diffusion tail for $\psi(t)$. It falls off more rapidly than $t^{-3/2}$ beyond $t/\tau = 5$, so that the area under the correlation analysis $\psi(t)$ actually exceeds the TDL one. However, it appears to be consistent with the correlation-function analysis over most of the range of times substantially involved in determining the linewidth. Also included in Fig. 4 are the results of two other calculations of $\psi(t)$: a microscopic analysis of the spin dynamics,[21] and a numerical calculation of spin correlations in a classical Heisenberg ferromagnet.[22] Both of

[19] P. G. de Gennes, J. Phys. Chem. Solids **4**, 223 (1958); W. Marshall, Natl. Bur. Std. (U. S.), Misc. Publ. No. 273, (1966).

[20] H, Mori and K. Kawasaki, Progr. Theoret. Phys. (Kyoto) **27**, 529 (1962); P. Resibois and M. De Leener, Phys. Rev. **152**, 305 (1966); **152**, 318 (1966).

[21] G. Reiter (unpublished). We are grateful to Dr. Reiter for discussions of his work prior to publication.

[22] C. G. Windsor, Proc. Phys. Soc. (London) **91**, 353 (1967). The results of this computer study of classical spin dynamics agree closely over the range of their validity with the results of Ref. 20.

these are in reasonable agreement with the forms of $\psi(t)$ determined here.

V. DISCUSSION

In the preceding three sections, we have explored, in some detail, alternate descriptions of strongly exchange-narrowed systems. In each case, we have used exact calculations of the leading terms in an expansion—namely, the first few moments of the line profile and the short-time behavior of the spin-correlation functions. We have been able to obtain more detailed information about these systems by examining one more term in each expansion than has been used heretofore and by making use of self-consistent comparisons between the line profile and correlation-function descriptions.

Within the restricted class of line shapes consistent with calculated second, fourth, and sixth moments, we have examined two model three-parameter profiles. Both of these give improved agreement with experiment over two-parameter forms fit to the second and fourth moments only. As we mentioned in Sec. III, it may at first seem unphysical that the best agreement with experiment is obtained using the abruptly terminated TDL shape, since it is clear that the spectrum of final states contributing to the absorption has no upper energy limit. However, if these states are separated into two-particle, three-particle, etc., classes, then each class is characterized by a well-defined upper energy bound. Furthermore, the usual phase-space restrictions lead to rapidly decreasing contributions from states of more than two particles, so that a sharp reduction in absorption at the maximum two-particle energy should be expected.[23] We believe that this is the physical origin of the sharp cutoff.

It is significant that the values of η for each profile are very similar in the NMR cases where M_2, M_4, and M_6 have been explicitly calculated, in spite of the fact that the strength of the broadening mechanism, the magnitude of the exchange, and the crystal structure are different in the rutiles and perovskites. This result is closely related to the observations of Sec. IV, where a study of the two leading coefficients of $\psi(t)$ indicated that the quantity β/α^2 also assumed a nearly constant value for all NMR cases investigated. In terms of the moments $\beta/\alpha^2 \cong M_2M_6/M_4^2$, while η for the three-parameter profiles has the form $\eta \propto M_4^2/M_2M_6$. Using the expressions appropriate for a magnetic nucleus (Eq. 2.13), we find that

$$\frac{M_2M_6}{M_4^2} = \frac{3}{2S(S+1)}\left[(4S^2+4S-1)\sum_j{}' J_{ij}^4+\tfrac{1}{3}S(S+1)\sum_{j\neq k} 14J_{ij}^2J_{ik}^2\right]/\left(\sum_j S_{ij}^2\right)^2, \tag{5.1}$$

where terms of the form $J_{ij}J_{ik}^2J_{jk}$ have been neglected in M_6 since they vanish for a two-sublattice antiferromagnet of the types discussed here. If a single-exchange interaction between neighboring spins is assumed, Eq. (5.1) reduces to the form $7-(2S^2-2S-3)/2zS(S+1)$. In that case, M_2M_6/M_4^2 is not dependent upon A, S, or J and has only a $1/z$ dependence upon the nature of the magnetic lattice. A similar weak dependence can be demonstrated for a partially magnetic nucleus.

The corresponding reduction of M_2M_6/M_4^2 is not possible in the EPR case because of the more complicated form of the dipolar interaction. However, if we assume a TDL line shape, we can find the appropriate value of η from M_2, M_4, and δ^{exp} [see Eqs. (3.7) and (3.8)]. The reasonably good linewidth prediction of TDL for EPR in $KMnF_3$ and $RbMnF_3$ (Table III) suggest that this is in fact a sensible model line shape. We have estimated η in this way for a number of materials ($KMnF_3$, $RbMnF_3$, MnF_2, EuO, EuS), and we find $0.08 \leq \eta \leq 0.2$. This relatively small range of values implies that the EPR line profiles in exchange-narrowed paramagnets are quite similar to one another; they are also very similar to the NMR shapes (where $\eta \approx 0.22$).

Our investigation of the moments has led us to a simple model profile for exchange-narrowed resonance lines which is physically plausible and is in substantial agreement with experiment. Our study of correlation functions using short-time expansions and a diffusion model for long times yield a form for $\psi(t)$ which is consistent with the line-shape analysis and is in agreement with the forms predicted from microscopic theory.[21] In the context of the preceding two paragraphs, we feel that these results may have more general application than to the three systems explicitly considered in this paper. Therefore, we believe that the current understanding of resonance in exchange-narrowed systems is comparable with that in nonmagnetic insulators.

ACKNOWLEDGMENTS

We are grateful to Professor P. Pincus for suggesting that more complicated lines be explored by calculating higher-order moments, and to Professor V. Jaccarino and Professor G. Reiter for their continued interest in this work and for many discussions concerning it.

[23] Such a cutoff is found in the work of Ref. 21, where three- and more particle final states have been neglected.